Eur. Phys. J. D **6**, 425–429 (1999)

THE EUROPEAN PHYSICAL JOURNAL D

EDP Sciences
© Società Italiana di Fisica
Springer-Verlag 1999

Scaling of hysteresis in a multi-dimensional all-optical bistable system

N. E. Fettouhi[a], B. Ségard, and J. Zemmouri[b]

Laboratoire de Spectroscopie Hertzienne de Lille, Centre d'Etude et de Recherches Lasers et Applications
Université des Sciences et de Technologies de Lille, 59655 Villeneuve d'Ascq Cedex, France

Received: 14 September 1998 / Received in final form: 15 February 1999

Abstract. We analyse the hysteresis enlargements of an optical bistable system involving three dynamical variables. We investigate, both experimentally and numerically, the local dynamics of the up- and down-switching process *versus* the sweeping frequency Ω of the control parameter. In particular, we delineate the domain of validity of the $\Omega^{2/3}$ scaling law predicted for one-dimensional systems. At high sweeping frequency, we show the appearance of another asymptotic scaling low in $\Omega^{1/2}$. Thereafter, we analyse the global evolution of the hysteresis loop induced by these processes. At low frequency, a $\Omega^{2/3}$ scaling law is retrieved, whereas at high frequency, the dynamical behaviour is shown to strongly depend on the particular shape of the bistability curve.

PACS. 42.65.−k Nonlinear optics – 42.65.Pc Optical bistability, multistability, and switching

If the static features of bistable systems are well established [1], their dynamical behaviours present some aspects relatively little known and subject to controversy [2]. It is the case of the enlargement of the hysteresis cycle of bistable systems submitted to a sweeping of one control parameter. Several studies of this phenomenon, both in deterministic (optical bistability) [3–5] and stochastic (magnetic hysteresis) [6–11] cases, have been performed leading to a scaling law giving the evolution of the hysteresis loops area as $Y_0^\alpha \Omega^\beta$. Y_0 and Ω are, respectively, the amplitude and the frequency of the control parameter modulation. The most interesting study carried out in this research area is a one-dimensional theory of dynamical hysteresis formulated by P. Jung *et al.* In this work, the authors show that the shift of the switching points and the hysteresis loops area scale as the two-thirds power of the sweeping frequency, in accordance with experimental results involving a bistable semiconductor laser [3]. In a multi-dimensional laser system, A. Hohl *et al.* examined scaling law of the bistable injected laser above and below threshold [4]. They demonstrated that the scaling exponent β is equal to 2/3 when the laser becomes bistable, the injected field being larger than the threshold. However, experiments [4,5] show that β decreases from 2/3 to much lower values when the sweeping frequency range increases. The origin of these behaviour remains not understood in so far as all the previous works mainly focus on the limit of relatively low sweeping frequencies.

In this paper, we investigate the hysteresis dynamics of an optical bistable device involving three dynamical variables on a much wider domain of sweeping frequency. In particular, we try to delineate the domain of validity of the $\Omega^{2/3}$ scaling law predicted for one-dimensional systems [3]. The dynamics of the up- and down-switching processes and the global evolution of hysteresis loop area are analysed. The influence of the characteristic time constants of the system on its dynamics is discussed.

The experiments were performed at a millimetre wavelength ($\lambda = 3.5$ mm). The experimental set-up, adapted from the arrangement extensively described in [12], consisted of a 23 m long waveguide Pérot-Fabry cavity filled with $HC^{15}N$ gas at low pressure. The source and the cavity were tuned to the frequency of the $J = 0 \rightarrow 1$ rotational line of $HC^{15}N$, which behaves as a saturable absorber (purely absorptive bistability). The sweeping of the input power is achieved by monitoring a PIN diode modulator. The output variable X and the control parameter μ are, respectively, the power transmitted by the cavity and the voltage applied to the modulator.

At low sweeping frequencies, when the system reaches a limit point A or B (see Fig. 1b), the trajectory of the bistable device in the plane (μ, X) jumps from one stable branch to another one giving rise to a static (or adiabatic) hysteresis loop (Fig. 1 a and b, (e)). If we keep unchanged the sweeping (frequency and amplitude) and increase the pressure, the static hysteresis width $(\mu_A - \mu_B)$ increases. Indeed the absorber saturation is reached for intra-cavity fields becoming higher and higher (Fig. 1 a, b, (e)) [12]. As the gas pressure considerably alters the static

[a] *Present address*: Université Moulay Ismail, Faculté des Sciences de Méknès, Morocco

[b] e-mail: jaouad.zemmouri@univ-lille1.fr

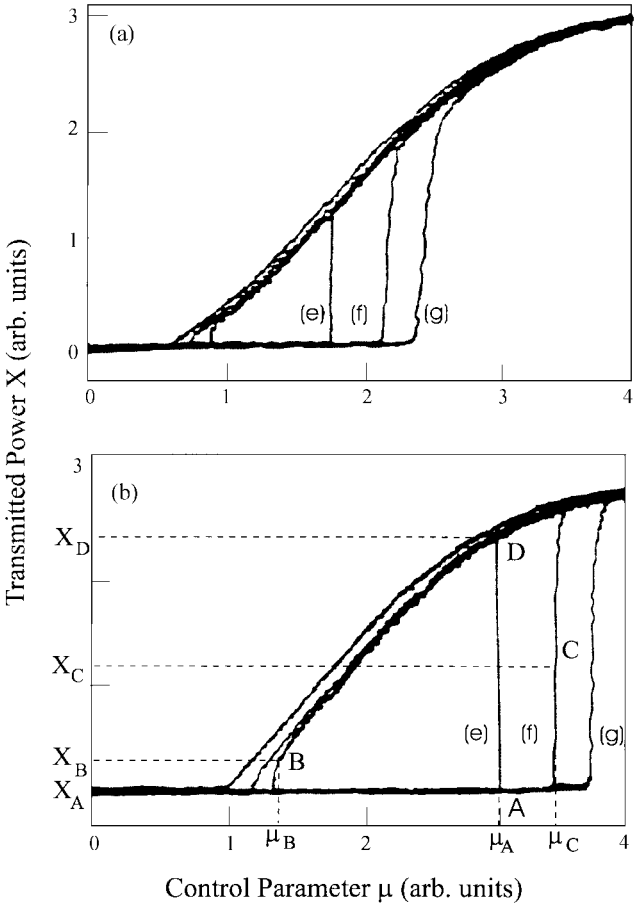

Fig. 1. Experimental evolution of the bistability curve *versus* the sweeping frequency of the input parameter for (a) low gas pressure (0.35 mTorr) and (b) high gas pressure (0.5 mTorr). Curves (e) obtained at 0.1 Hz give a good approximation of the static loop. Curves (f) and (g) are, respectively, obtained at 100 Hz and 500 Hz.

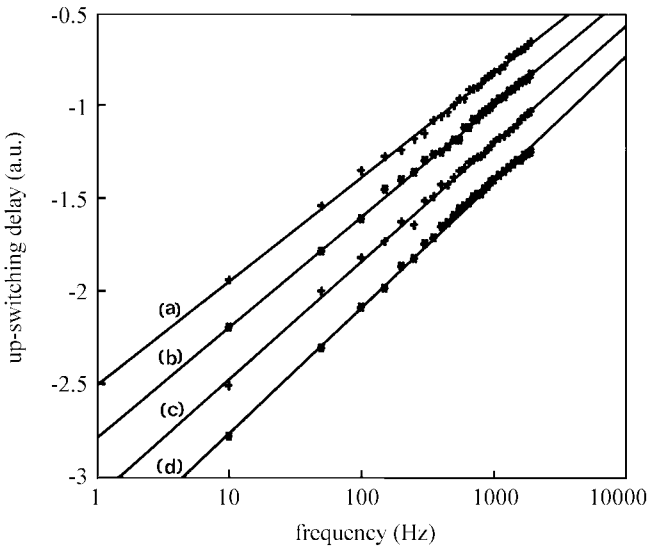

Fig. 2. Experimental evolution of the up-switching delay *versus* the sweeping frequency for different pressures (log-log plot). Pressure = (a) 0.35 mTorr, (b) 0.45 mTorr, (c) 0.55 mTorr, and (d) 0.65 mTorr. The straight lines are obtained by a least-square fit.

characteristic of our bistable device, we can conjecture that it plays a role in its dynamic. We have studied the evolution of the hysteresis loop characteristics (switching points position and loop area) *versus* the sweeping frequency for different gas pressure. In this experiment, a sinusoidal modulation signal is applied to the modulator in addition to a bias current. The amplitude of each of them is adjusted in order to modulate the input power from zero to its maximum available value. The sweeping frequency varies from 10 Hz to 2000 Hz.

Due to the experimental limitations, the gas pressure actually reachable varies from 0.3 to 0.7 mTorr. At lower pressure, the bistable domain vanishes whereas for pressure larger than 0.7 mTorr the frustration phenomenon [13] appears at high sweeping frequencies and strongly modifies the loop shape. Despite the narrowness of our experimental pressure range, it has been possible to show an indisputable influence of the pressure on the hysteresis dynamics. Figure 1 shows the evolution of the hysteresis loop *versus* the sweeping frequency for low (Fig. 1a) and high pressure (Fig. 1b). Increasing the driving frequency, the hysteresis loop becomes larger since the switching points are delayed (Fig. 1 a, b, (f), (g)) [3].

As in [5], the definition of the up-switching points (μ_C) is different from the criterion used in [3]. In this work, the switching point is defined as the value of the input control parameter for which the output variable is equal to the ordinate X_A of the limit point A. In our system, the switching point is defined as the control parameter for which the output variable is equal to $(X_A + X_D)/2$ (X_D is the ordinate of the point D of the upper branch whose abscissa is μ_A (Fig. 1 b, (e)). The choice of this criterion is imposed by the fact that our bistable system involves three dynamical variables. Indeed, for relatively high sweeping frequencies, the numerical simulations on a three-dimensional model have shown that the trajectories observed during the forward sweep can cross the lower branch of the bistability cycle and reaches X_A before the control parameter reaches μ_A. In addition, experimentally X_A is of the same order than the experimental noise. In the following we will see that, as indicated in reference [5], the criterion for the switching point slightly modifies the value of the exponent β obtained for a given pressure. Nevertheless, the global evolution of β with pressure does not significantly depend on the criterion in the condition of our experiments and simulations.

Figure 2 shows, in log-log plot, the evolution of the switching delay ($\mu_C - \mu_A$) *versus* frequency for different gas pressures in the case of the up-switching process. The straight lines are obtained by a least-square fit. The abscissa μ_A of the turning point A is first approximated by the value of μ_C measured at very low sweeping frequency ($\Omega/2\pi = 0.1$ Hz) and then slightly adjusted in order to achieve the best fit. The slope of the straight lines gives the exponent β characterising the evolution of the switching delay *versus* the sweeping frequency. The evolution of

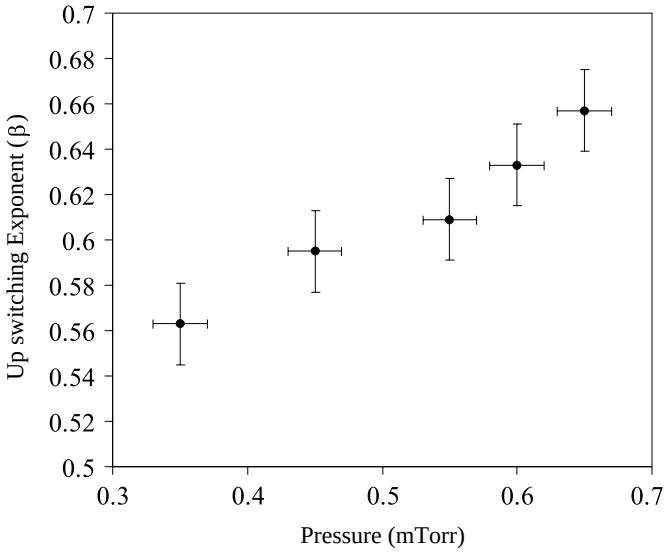

Fig. 3. Evolution of the scaling law exponent β *versus* the gas pressure for the up-switching process: experimental result.

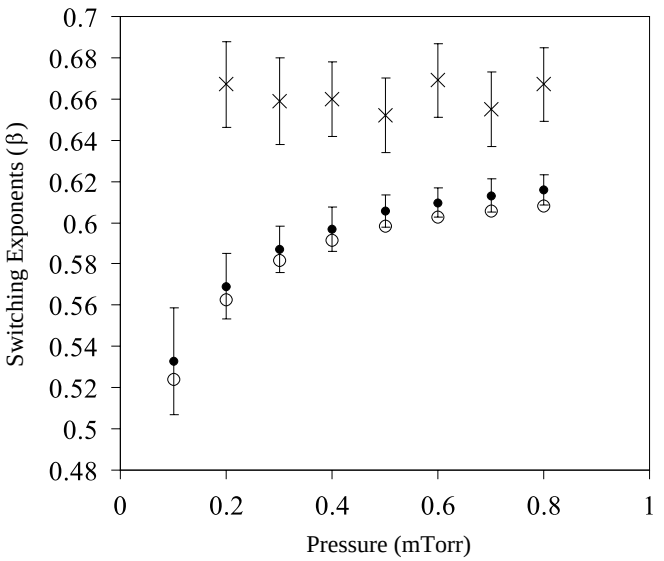

Fig. 4. Evolution of the exponent β with pressure obtained by numerical simulation in the conditions of Figure 3. Cross: down-switching process; Dot and circle: up-switching process (Dot and circle, respectively, correspond to two different criteria for switching point).

β *versus* the pressure is plotted in Figure 3. The errors on β, equal to three times the standard deviation given by the fit, are close to 0.02. This value is much smaller than the variation of β observed in the figure. β clearly depends on the gas pressure and increases from 0.56 to 0.65 when the pressure increases from 0.35 mTorr to 0.65 mTorr. Let us emphasise that the value of β obtained for higher gas pressure is very close to the theoretical value 2/3 predicted in the one-dimensional model [3]. In the particular case of our bistable system, the ordinate X_B of the turning point B is too low to allow precise measurement of the down-switching point positions.

For numerical simulation, our bistable device has been modeled by an equivalent ring cavity [12] of twice length with two identical mirrors filled with a homogeneously broadened two-level medium. Limiting our study to the purely absorptive bistability [14], we can expect that in our experiments, the dynamics of our system involves only one mode of the cavity. Consequently, a single mode model in the plane-wave approximation should provide a good basis for the theoretical description of our experiments. The Maxwell-Bloch equations that govern the dynamics of systems with saturable absorber then write

$$\begin{aligned} \tau_{\rm ph}\frac{{\rm d}F}{{\rm d}t} &= Y - F - 2CP\,, \\ T_2\frac{{\rm d}P}{{\rm d}t} &= FD - P\,, \\ T_1\frac{{\rm d}D}{{\rm d}t} &= FP + D - 1\,. \end{aligned} \tag{1}$$

F is the normalised slowly varying envelope of the intracavity field, defined by $F = 2\pi\nu_{\rm r}\sqrt{T_1T_2}$, where $\nu_{\rm r}$ is the Rabi frequency of this field. The input field is defined by $Y = \frac{2\pi\nu_{\rm ri}}{\sqrt{T}}\sqrt{T_1T_2}$, where $\nu_{\rm ri}$ is the Rabi frequency of the input field and T the mirror transmittivity. D and P are the normalised slowly varying envelopes of the population difference and of the molecular polarisation, respectively.

T_2 and T_1 are the relaxation times of the polarisation and population difference, respectively. The relaxation mechanism of the rotational transitions is essentially collisional and may be generally characterised by a unique relaxation time ($T_2 = T_1$) inversely proportional to the pressure and equal to 7 μs at 1 mTorr. The cavity photon lifetime $\tau_{\rm ph}$ is directly linked to the cavity mode width. $C = \alpha L/2(1-R) = 200$ is the bistability parameter where α is the power absorption coefficient of the absorber, R is the reflection coefficient of the cavity mirrors and L is the Fabry-Perot cavity length. R and T have been measured and are respectively equal to 0.96 and 0.015 ($R+T \neq 1$). As in reference [12], α is taken equal to 0.8 m^{-1}. The input field is sinusoidally swept from zero to Y_0 as $Y = Y_0$ $(1 - \cos\Omega t)/2$. Unfortunately, contrary to reference [12], the calculated values of the static cycle width (in unit of μ_A) are 1.5 time larger than those measured in experiments. This discrepancy between experiment and theory is mainly due to the inhomogeneous broadening linked to the Doppler effect which noticeably influences the gas transmission at our working pressure.

In the numerical calculations, the input field Y is taken as the control parameter and the conditions are as close as possible to the experimental one for which the maximum of input power remains fixed whatever the value of the pressure. In these conditions, the value of the reduced parameter Y_0 evolves as the inverse of the pressure. Contrary to the experiments, the analysis of the dynamics near the down-switching point B (Fig. 1b) is feasible. Figure 4 shows the evolution of the exponent β *versus* pressure for the two switching processes. As in experiments, the values of β are obtained by a least-square fit, but the parameter μ_A (μ_B for the down-switching process), analytically known, is not adjusted. The error bars correspond to three

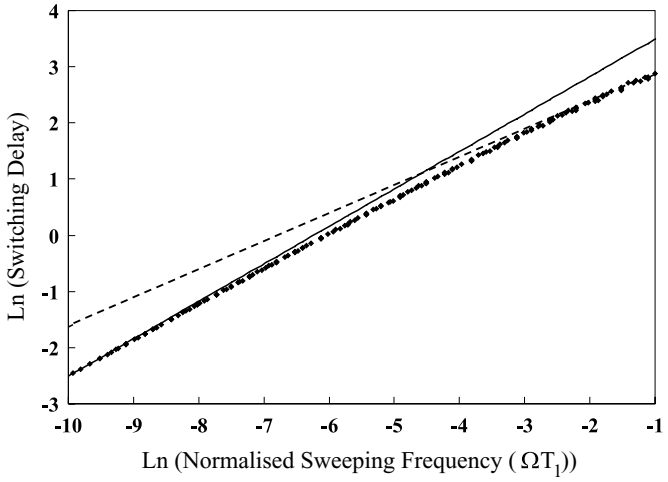

Fig. 5. Evolution of the switching delay *versus* the normalised sweeping frequency (log-log plot). The straight lines indicate the asymptotic behaviours. Their slopes are, respectively, equal to 2/3 (full line) and 1/2 (dashed line).

standard deviations. For the up-switching, the evolution of β is similar to that observed in the experiments. In the range 0.1 to 0.8 mTorr, β increases with the pressure from 0.53 to 0.62. These values are smaller than the experimental one but the deviations do not exceed twice the experimental errors. The theoretical value 0.66 is reached for higher pressures and lower sweeping frequencies. This difference between experiments and numerical simulations could be imputable to the roughness of the theoretical model and also to the non-linearity of the input modulation which can reduce the sweeping velocity in the vicinity of the turning point A for high pressures. Let us point out that the values of β marked by circles in Figure 4 are obtained by using the value $(X_A + X_D)/8$ as criterion for the switching point. The modifications, induced by this change of criterion, are of the same order of magnitude as the errors. The evolution of β is not significantly modified, the theoretical value 2/3 is only reached for lower frequencies.

Contrary to the up-switching process, the exponent β for the down-switching remains close to the theoretical value 2/3 and does not depend on the pressure. It appears therefore that the switching dynamics of our system depends on the considered switching process. In the vicinity of the turning point A where the intra-cavity field is close to 0, the dynamics is dominated by the population difference D [15] and the characteristic time is T_1. The evolution of the exponent β evidenced both experimentally and numerically, simply indicates that as the pressure decreases, T_1 increases and the normalised sweeping frequency ΩT_1 becomes higher and higher. In this way, the bistable system leaves progressively the validity domain of the one-dimensional scaling law ($\beta = 2/3$). At high normalised frequencies (low pressures), the exponent β strongly depart from the theoretical value 2/3. This behaviour is in good agreement with the experimental results of reference [4], which show that the scaling exponent β decreases from 0.62 to 0.52 when the upper limit of the sweeping frequency domain increases. In order to precise the evolution of β at highest normalised sweeping frequency, we have undertaken another series of numerical simulations for which the reduced parameter Y_0 is held constant and is twice the value of the input parameter Y at the turning point A. The normalised sweeping frequency (ΩT_1) is varied in a wide domain (2×10^4 factor). The corresponding evolution of the switching delay is graphed in Figure 5. At low sweeping frequency, we retrieve the 2/3 exponent law (full line), whereas the curve shows an other asymptotic behaviour at high normalised frequencies. The delay then evolves as $\Omega^{1/2}$ (dashed line). This last behaviour can be explained as follows. At high sweeping frequency, the switching occurs far from the turning point, so that we can conjecture that it is ruled by a pulse area law [16–18] and occurs when the area swept by the control parameter μ ($\mu = Y$ here) reaches a value A_0 which only depends on the state of the bistable system at the beginning of the sweeping. In the frame of the linearised model developed in reference [3], μ is linearly swept at a velocity $v \sim \Omega T_1$. The switching then occurs after a time duration t given by

$$A_0 = vt^2/2\,. \tag{2}$$

The corresponding value of the control parameter μ_C writes

$$\mu_C = vt + \mu 0\,, \tag{3}$$

where μ_0 is the initial value of the control parameter. Equations (2) and (3) lead to

$$\mu_C - \mu_A = \sqrt{2A_0 v} + \mu_0 - \mu_A\,. \tag{4}$$

It appears that for large value of the sweeping velocity, the switching delay $(\mu_C - \mu_A)$ evolves as $v^{1/2}$ *i.e.* as $\Omega^{1/2}$. We then retrieve the asymptotic law evidenced by our numerical simulation. Complementary numerical simulations, performed on the generic one-dimensional model of reference [3] and using the criterion defined by the authors, also show the existence of two asymptotic laws, respectively, characterised by $\beta = 2/3$ and $\beta = 1/2$. These two laws, evidenced in one- and three-dimensional models are expected to be valid for any bistable device. Depending on the characteristics of the bistable system under consideration (time constant and sweeping frequency domain), the values of β can vary from 0.5 (high normalised frequencies) to 0.66 (low normalised frequencies). For instance, for a given range of sweeping frequencies, an increase in the characteristic time constant entails a shift of the normalised frequency range from the domain of validity of the $\Omega^{2/3}$ scaling law toward that of the $\Omega^{1/2}$ law and therefore a decrease of β. This can explain the spread of the values of β obtained in previous works [4,5].

Concerning the down-switching process in our optical bistable device, the master variable is the intra-cavity field [15], the characteristic evolution time is $\tau_{\rm ph}$ and the normalised frequency $\Omega\tau_{\rm ph}$ does not depend on pressure, so that the exponent β does not significantly vary with pressure. In addition, for our particular conditions, the normalised frequencies are small enough to remain in the validity domain of the $\Omega^{2/3}$ law. Obviously, if we could

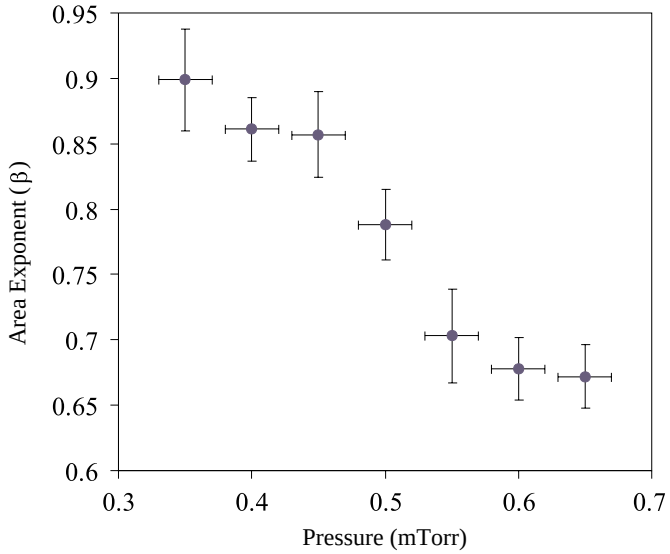

Fig. 6. Evolution, *versus* pressure, of the exponent β characterising the area enlargement: experimental result.

increase the photon lifetime $\tau_{\rm ph}$ the exponent β would be smaller.

Except for one-dimensional system, the up- and down-switching process of bistable systems are generally characterised by different time constants and the evolution of the switching delay *versus* the sweeping frequency can differ from one process to the other. On the other hand, for a given process the experimental value of the exponent β of the scaling law could vary from 2/3 to 1/2 according to the time constant value and the sweeping frequency range experimentally used.

All the previous behaviours will affect considerably the dynamics of the hysteresis loop area. The corresponding experimental results are resumed in Figure 6 in which the exponent β, characterising the area enlargement, is graphed *versus* the pressure. β decreases from 0.9 to approximately 2/3 when the pressure increases from 0.35 to 0.65 mTorr (Fig. 6). At high pressure (low normalised frequency) the area dynamics is ruled by the theoretical law predicted in the framework of a one-dimensional model but our results strongly depart from this law at low pressure (high normalised frequency). In this last condition, the area enlargement roughly increases linearly with the sweeping frequency. We claim that this behaviour is linked to the particular shape of the bistability curve of our device. Figure 1 shows that the area enlargement is mainly due to the up-switching point displacement. The increase of the loop area corresponds to the trapezium limited by the curves (e) (static hysteresis) and (f) of Figure 1 whose area ΔA can be written:

$$\Delta A = a(\mu_{\rm C} - \mu_A) + b(\mu_{\rm C} - \mu_A)^2 \,. \qquad (5)$$

At low frequency (small delay $\mu_{\rm C} - \mu_A$) the first term prevails and ΔA is proportional to $\Omega^{2/3}$. At high sweeping frequency the second term becomes predominating, as $\mu_{\rm C} - \mu_A$ is then proportional to $\Omega^{1/2}$, ΔA increases linearly with the sweeping frequency Ω. Let us emphasise that this linear evolution is specific to absorptive optical bistable systems for which the output variable is nearly proportional to the input parameter when the system visits the upper branch of its bistability cycle. In fact, the dynamics of bistable hysteresis area at high sweeping frequencies depend on the particular shape of its characteristic curve. On the contrary, at low frequencies the $\Omega^{2/3}$ law is expected to hold whatever the bistable device.

In conclusion, our study of the hysteresis dynamics in an optical bistable system involving three dynamical variables has shown that this dynamics depends on the nature of the master variable that governs the time evolution of the system near the limit point. Basically, for a given sweeping frequency, the characteristic time constant, corresponding to this master variable, drives the dynamics. At low normalised frequencies, the switching delay evolves as $\Omega^{2/3}$ whereas at high frequency the $\Omega^{1/2}$ scaling law prevails. On the other hand, the global evolution of the hysteresis loop area linked to the local evolution near the turning points follows a $\Omega^{2/3}$ law at low sweeping frequencies, but the scaling law strongly depends on the shape of the static hysteresis loop at high frequencies.

The Laboratoire de Spectroscopie Hertzienne is "Unité Associée au CNRS". The Centre d'Etude et de Recherches Lasers et Applications (CERLA) is supported by the Ministère chargé de la Recherche, the region Nord/Pas de Calais and the Fonds Européen de Développement Economique des Régions.

References

1. R. Bonifacio, L. A. Lugiato, Opt. Commun. **19**, 172 (1976).
2. M. Rao, Phys. Rev. Lett. **68**, 1436 (1992). P. Jung, G. Gray, R. Roy, P. Mandel, Phys. Rev. Lett. **68**, 1437 (1992).
3. P. Jung, G. Gray, R. Roy, P. Mandel, Phys. Rev. Lett. **65**, 1873 (1990).
4. A. Hohl, H. J. C. van der Linden, R. Roy, G. Goldsztein, F. Broner, S.H. Strogatz, Phys. Rev. Lett. **74**, 2220 (1995).
5. J. Grohs, H. Ibler, C. Klingshirn, Opt. Commun. **86**, 183 (1991).
6. M. Rao, H. R. Krishnamurty, R. Pandit, Phys. Rev. B **42**, 856 (1990).
7. M. Rao, H. R. Krishnamurty, R. Pandit, J. Appl. Phys. **67**, 5451 (1990).
8. Y. L. He, G. C. Wang, Phys. Rev. Lett. **70**, 2336 (1993).
9. W. S. Lo and R. A. Pelcovits, Phys. Rev. A **42**, 7471 (1990).
10. S. Senjupta, Y. Marathe, S. Puri, Phys. Rev. B **45**, 7828 (1992).
11. Z. Fan, Z. Jianxiu, L. Xiao, Phys. Rev. E **52**, 1399 (1995).
12. B. Ségard, B. Macke. L. A. Lugiato, F. Prati, M. Brambilla, Phys. Rev. A **39**, 703 (1989).
13. J. Zemmouri, B. Ségard, W. Sergent, B. Macke, Phys. Rev. Lett. **70**, 1135 (1993).
14. L. A. Lugiato, *Progress in Optics*, edited by E. Wolf, Vol. **21** (1984).
15. T. Erneux, P. Mandel, Phys. Rev. A. **28**, 896 (1983).
16. F.A. Hopf, P. Meystre, Opt. Commun. **29**, 235 (1979).
17. P. Mandel, Opt. Commun. **55**, 293 (1985).
18. B. Ségard, J. Zemmouri, B. Macke, Opt. Commun. **60**, 323 (1986).